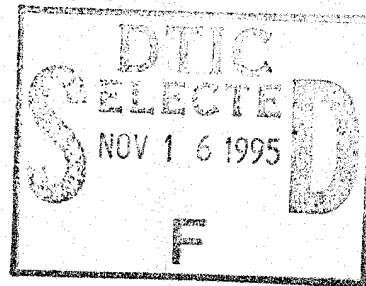


D440682

1586005863
L1-10567-M9

Los Alamos National Laboratory is operated by the University of California for the United States Department of Energy under contract W-7405-ENG-36.



19951114 106

Load-Rate Characteristics of Certain Polyurethane Foams

DEPARTMENT OF DEFENSE
PLASTICS TECHNICAL EVALUATION CENTER
ARRADCOM, DOVER, N. J. 07801

DTIC QUALITY INSPECTED 8

Los Alamos Los Alamos National Laboratory
Los Alamos, New Mexico 87545

Approved for public release
Distribution Unlimited

PLASTED 49974

DISCLAIMER

This report was prepared as an account of work sponsored by an agency of the United States Government. Neither the United States Government nor any agency thereof, nor any of their employees, makes any warranty, express or implied, or assumes any legal liability or responsibility for the accuracy, completeness, or usefulness of any information, apparatus, product, or process disclosed, or represents that its use would not infringe privately owned rights. Reference herein to any specific commercial product, process, or service by trade name, trademark, manufacturer, or otherwise, does not necessarily constitute or imply its endorsement, recommendation, or favoring by the United States Government or any agency thereof. The views and opinions of authors expressed herein do not necessarily state or reflect those of the United States Government or any agency thereof.

LA-10567-MS

UC-25

Issued: November 1985

Load-Rate Characteristics of Certain Polyurethane Foams

Elton G. Endebrock

DTIC-AE <i>etc</i>	
Dist Period <i>11-2-95</i>	
Availability Codes	
Dist	Avail and/or Special
<i>A-1</i>	

LOAD-RATE CHARACTERISTICS OF CERTAIN POLYURETHANE FOAMS

by

Elton G. Endebroek

ABSTRACT

Three urethane foams were subjected to quasistatic and drop tests to evaluate their mechanical properties under various loading rates. The foam formulations, tests, and data reduction procedures are described and test results are presented and discussed. All of the foams are load-rate sensitive and have large energy absorbing capacities when loaded beyond their yield stresses.

I. INTRODUCTION

This test program was initiated to determine the mechanical properties of certain polyurethane foams under dynamic conditions and is a part of a greater effort directed towards evaluating polyurethane foams for use in specific applications. The information from these tests will provide a more rational method for selecting a particular polyurethane foam formulation for a specific application.

Because the intended applications involve impact loadings, the behavior of the foams when subjected to larger than usual loading rates is of special interest. Compressive tests with loading rates up to 9000 mm/min are possible using hydraulic universal testing machines. For higher loading rates, a drop test was used. This drop test produces loading rates of 80 000 mm/min and higher. The load rate of 80 000 mm/min is equivalent to a strain rate of 52.5 1/s for samples that are 25.4 mm in height. Currently we do not have a test apparatus for loading rates between 9000 and 80 000 mm/min. The drop test and data reduction techniques especially developed for this test program are described in subsequent sections.

II. MATERIAL DESCRIPTION

In this investigation, polyurethane foam samples of three different formulations were tested. Polyurethanes are formed by the reaction of isocyanate (catalyst) with a resin. The resin is a saturated polyester or polyether.

Two of the polyurethane foams tested belong to the Stafoam 760 system. This is a polyurethane system manufactured by the Expanded Rubber and Plastics Corporation. This system contains a polyester based resin that reacts with isocyanate to polymerize and cross-link.

Carbon dioxide is produced by the reaction of water and carboxylic acid with the isocyanate. When the carbon dioxide is released, the material expands as gelling occurs, thus forming a rigid foam. These foams are identified in this report as 30 (density 0.48) and 40 (density 0.64) pcf foams.

The third foam is "Sunshine" foam, which is a syntactic foam manufactured by incorporating glass microballoons into a polyurethane elastomer. The elastomer system used is Uralite 3121S, which is manufactured by the Hexcel Corporation. It contains a polyether based resin and undergoes a polyol cure with aromatic diisocyanate.

Table I lists the foam components, expressed as a percentage of the total weight, along with the foam densities.

TABLE I
FOAM COMPONENTS AND DENSITY

Components (% by Weight)	Item	Foam		
		Sunshine	30 Pcf	40 Pcf
Resin		24.86	56.02	56.67
Catalyst		62.14	43.83	43.26
Water		0.0	0.15	0.07
Glass Microballoons		13.0	0.0	0.0
Density				
kg/m ³		660	430	610
lbs/ft ³		41.2	26.8	37.9

III. DROP TEST AND DATA MEASUREMENT DESCRIPTION

A. Test Description

A test for obtaining the effects of loading rates on materials requires a moving device that impacts a material sample. A simple device for delivering energy to a material sample is a weight dropped from some height.

A drop test set-up is illustrated in Fig. 1. The strain rate is proportional to both the impact velocity and sample height, and the drop weight and height combination determines the maximum force (and energy) applied to the material sample. The usual procedure is to select the drop height to obtain a selected velocity and then determine the weight based on the energy at impact. The test results reported here were obtained using the drop tower in Building TA-16-54.

Test responses were measured using two accelerometers attached to the drop weights. Actually, only one accelerometer is required, the second one acts as a back-up. The response accelerograms were captured on a Nicolet digital oscilloscope. The impact velocities were not measured, but were computed based on the drop height and the acceleration of gravity adjusted for the test site elevation. The computed impact velocities were decreased by 1% to account for estimated friction losses.

The drop test data were recorded on diskettes and later transmitted to a VAX 11/780 computer for conversion to more usable and familiar forms.

B. Data Reduction

1. Measured Accelerogram Characteristics and Noise. The measured accelerograms include additional higher frequencies (ringing) superimposed on the primary response pulse as illustrated in Fig. 2. These higher frequencies occur in the drop weight, the material sample, and the anvil because of mechanical imperfections and the sudden impacting of the drop weight onto the material sample. In some cases, the ringing amplitudes are large enough to mask the shape of the primary pulse. Also, this ringing presents problems in determining the maximum amplitude of the primary pulse and causes difficulties in interpreting the reduced data. Adjustments in the test procedures and hardware may decrease the ringing amplitudes, but the ringing cannot be eliminated without filtering.

The velocities are obtained by integrating the accelerograms and the displacements are obtained by integrating the velocities. The initial velocity is the velocity of the dropping weight at the instant of impact. Because the initial velocity is not zero, the displacements will be inaccurate unless the zero time point of the primary acceleration pulse is accurately selected. The zero time point is calculated based on the intersection of the signal base line and the initial slope of the signal. A manual selection is available if the calculational method fails.

2. Data Reduction Using Computer Programs. A computer program was developed to aid in reducing the test data. This program is interactive and computational functions are selected from a menu. This program performs the following functions:

a. Plots accelerograms. Axis limits are either user supplied or calculated by the program.

b. Computes and plots power spectral density function (PSD) of accelerograms. The PSD is an aid in the selection of filter parameters.

c. Filters (or smooths) accelerograms using a Butterworth low-pass digital filter. Used to remove the unwanted higher frequencies from the accelerograms.

d. Computes zero time point of primary pulse. Also allows manual input of zero time point in case the program does not adequately determine the starting point.

e. Computes quantities such as the maximum acceleration, equivalent viscous damping coefficient, average velocity during loading of the material sample, and the area enclosed by the stress-strain curve during a loading and unloading cycle to be computed.

Figure 3 shows a measured accelerogram. The PSD of this signal, which is shown in Fig. 4, yields the signal's frequency content. The frequency content of the primary acceleration pulse ranges from 0 to about 2500 Hz. Frequencies above this result from noise and/or ringing. Note that the frequency of 16 300 Hz can be identified with ringing (sound wave reflecting back and forth) in the drop weight. After examination of the PSD in Fig. 4, a filter cutoff frequency of 4000 Hz was selected. Figure 5 shows the Fig. 3 accelerogram after being filtered (or smoothed). Note that the higher frequencies have been removed and that the appearance of the primary acceleration pulse has been greatly enhanced. The PSD plot (Fig. 6) of the filtered accelerogram also illustrates that the higher frequency effects have been removed without altering the magnitude and shape of the primary pulse.

Whenever a signal is captured on a digital oscilloscope, the zero time point indicated by the oscilloscope normally does not correspond to the starting time of the signal. For data analysis, it is therefore necessary to shift the time axis such that the zero time point coincides with the start of the signal. Figure 7 shows the Fig. 5 accelerogram time shifted to the start of the acceleration pulse.

After the accelerograms have been filtered and time base corrected, the program QKPLT is used to compute and display the stress-strain relationship and to compute the modulus of elasticity. The stress-strain relationship obtained from the Fig. 7 accelerogram is shown in Fig. 8. To obtain the modulus of elasticity, time and strain limits are manually selected. These limits are therefore determined by the judgment of the analyst.

IV. TESTS AND DISCUSSION OF RESULTS

A. Quasistatic Tests

Quasistatic tests were conducted for loading rates of 10, 50, 100, 500, and 9000 mm/min (0.0066, 0.0328, 0.0656, 0.3280, and 5.9100 1/s). The tests and test results for each foam are presented in Table II.

The differences in the moduli of elasticity for the 40 pcf foam loaded at a rate of 0.0066 1/s (10 mm/min) give an indication of the sample-to-sample variation that may be expected. Typical load-deflection relationships for each foam are shown in Figs. 9-11. Yield stresses were obtained using the offset method. For all foams, an offset strain of 2.0% was used.

In all of the quasistatic tests, the material samples were loaded to a strain of 40% or higher. As is evident from the load-deflection curves in Figs. 9-11, the 30 and 40 pcf foams were permanently deformed; however, the Sunshine foam showed little permanent deformation. Any permanent deformation in the Sunshine foam is not visibly noticeable. For samples tested at loading rates up to 0.328 1/s (500 mm/min), none of the foam samples displayed fracture lines; however, both the 30 and 40 pcf foam samples displayed fracture lines when tested at a loading rate of 5.91 1/s (9000 mm/min) up to a maximum strain of about 60%.

TABLE II

QUASISTATIC TEST RESULTS

<u>Strain Rate (1/s)</u>	<u>Yield Stress (MPa)</u>	<u>Modulus of Elasticity (MPa)</u>
<u>Sunshine Foam</u>		
0.0066	7.2	137
0.0066	7.7	132
0.0656	8.9	176
0.0656	9.3	176
0.3280	11.6	161
5.9100	15.9	259
<u>30 Pcf Stafoam 760</u>		
0.0066	12.3	265
0.0066	12.0	308
0.0656	12.3	398
0.0656	12.7	353
0.3280	14.4	236
0.3280	14.0	245
5.9100	18.3	413
5.9100	15.5	334
<u>40 Pcf Stafoam 760</u>		
0.0066	33.9	695
0.0066	23.7	479
0.0066	22.1	745
0.0328	10.5	253
0.0328	11.5	287
5.9100	30.4	609
5.9100	28.8	634

B. Low Impact-Energy Tests

The first series of drop tests was conducted using one 30 pcf foam sample. The purposes of these tests were to verify that the test procedures were adequate and that the data transmission-reduction sequence functioned as planned. Low impact-energy tests were conducted such that the same material sample could be used in successive tests.

A weight of 2.68 kg (5.91 lbs) was dropped from heights of 0.381 m (15 in.), 0.635 m (25 in.), and 0.254 m (10 in.). Results of these tests are summarized in Table III. Because these tests were conducted on the same day

(February 11, 1985), any aging effects are eliminated. Considering Table III, there appears to be a trend toward greater yield stresses and moduli of elasticity as the impact velocity increases. Judging from the yield stresses, moduli of elasticity, and maximum displacements, it appears that the sample was damaged during the first drop test from 0.635 m (Test 4). Tests 1-2 and 6-7 show small test-to-test variation in moduli of elasticity, yield stresses, and displacements. Recall that aging effects were eliminated from these tests.

The acceleration pulse for Test 1 (Table III) is shown in Fig. 12. The near symmetry of this pulse, as indicated by the rise and decay times, signifies that the material responded in a near linearly-elastic manner. For a perfectly linear material, the acceleration pulse is symmetric. The acceleration pulse for Test 4 is shown in Fig. 13. Note that the rise and decay times are somewhat different thereby indicating that some inelastic action has occurred.

The stress-strain relationship obtained from Test 1 is shown in Fig. 14. Hysteresis is evident even though the foam sample responded in a near elastic manner. Most of the hysteresis is because of damping, which is always present in dynamic responses. The stress-strain relationship will display hysteresis even for perfectly linear materials.

TABLE III

LOW IMPACT-ENERGY TESTS ON 30 PCF FOAM

Drop Weight - 2.68 kg

Test No.	Drop Height (m)	Maximum Displacement (mm)	Impact Velocity (m/s)	Yield Stress (MPa)	Modulus of Elasticity (MPa)	Initial Strain Rate (1/s)
1	0.381	1.41	2.702	14.7	366	107
2	0.381	1.49	2.702	14.9	369	107
3	0.381	1.44	2.702	14.7	355	107
4	0.635	1.62	3.489	18.1	379	139
5	0.635	1.67	3.489	17.8	356	139
6	0.254	1.10	2.206	11.9	337	88
7	0.254	1.17	2.206	12.1	341	88
8	0.635	1.74	3.489	17.2	328	139

C. Drop Tests On New Material Samples. After the low impact-energy tests had been completed, weights of 5.56 kg (12.25 lbs), 10.05 kg (22.15 lbs), and 19.24 kg (42.42 lbs) were obtained. This permitted a test series in which the drop heights (and impact velocities) could be varied, but the impact energy maintained at a near constant value. Exploratory tests to determine an energy level that would fracture one of the foams were undertaken. An

impact energy of about 3.15 MJ/m³ (458 in.-lb/in.³) fractured a 40 pcf foam sample. Drop weights and heights for the next test series were therefore selected based on this energy value.

The results of the tests with impact energies of about 3.15 MJ/m³ are given in Table IV. The area factor is the ratio of the area enclosed by the stress-strain curve during a load and unload cycle divided by the product of the maximum stress times the maximum strain. This quantity is a measure of the energy lost to inelastic action.

TABLE IV

RESULTS OF DROP TESTS ON NEW SAMPLES

Impact Energy - 3.15 MJ/m³

<u>Initial Strain Rate (1/s)</u>	<u>Area Factor</u>	<u>Maximum Strain (mm/mm)</u>	<u>Yield Stress (MPa)</u>	<u>Modulus of Elasticity (MPa)</u>	<u>Test Date</u>
<u>Sunshine Foam</u>					
213	0.605	0.156	30.2	599	02-25-85
213	0.580	0.145	29.9	598	02-28-85
166	0.606	0.162	28.9	551	03-08-85
120	0.611	0.156	29.0	626	04-02-85
120	0.593	0.147	32.0	651	04-03-85
<u>30 Pcf Stafoam 760</u>					
213	0.566	0.150	24.6	477	02-25-85
166	0.685	0.184	17.9	850	03-08-85
166	0.700	0.202	17.8	327	03-18-85
120	0.636	0.165	23.2	406	04-02-85
120	0.692	0.187	19.0	406	04-03-85
<u>40 Pcf Stafoam 760</u>					
213	0.532	0.120	32.9	614	02-28-85
166	0.590	0.127	33.2	625	03-08-85
166	0.558	0.121	36.4	681	03-18-85
120	0.557	0.127	32.6	571	04-02-85
120	0.474	0.103	42.4	818	04-03-85

Only the 40 pcf foam samples displayed visible fractures after the first impact. Chips and segments separated from the 40 pcf foam samples during several tests. Recall that in the quasistatic tests, the 40 pcf foam did not fracture for deformations up to one-half of the sample's original height.

An examination of the results presented in Table IV leads to the following observations:

1. The parameter with the smallest test-to-test variation is the yield stress.

2. The parameter with the greatest test-to-test variation is the modulus of elasticity. Because of large deviations from the average, mistakes in testing or data reduction were suspected. These cases were carefully investigated and no mistakes were found. The modulus of 818 MPa for the 40 pcf foam could be due to sample-to-sample material difference because the yield stresses, area factor, and maximum strain also differ from their respective comparable values. The modulus of 850 MPa for the 30 pcf foam is a mystery because the other parameters do not differ from their comparable values.

3. The lack of data precludes a firm conclusion, but it appears that the yield stress and modulus of elasticity increase with the age of the foam.

4. The average area factors for the 30 pcf, Sunshine, and 40 pcf foams are 0.656, 0.599, and 0.535, respectively.

5. The average yield stresses for the 40 pcf, Sunshine, and 30 pcf foams are 35.3, 30.0, and 20.5 MPa, respectively.

6. The average moduli of elasticity for the 40 pcf, Sunshine, and 30 pcf foams are 654, 605, and 493 MPa, respectively.

Stress-strain relationships for Sunshine, 30 pcf, and 40 pcf foams are shown in Figs. 15-17. These stress-strain curves were obtained from first impact tests with the same impact energy. Only Sunshine foam (Fig. 15) displays a strain softening region. All of the foams have high energy absorption capabilities as indicated by the area enclosed within the stress-strain curves.

D. Repeated Impact Tests

If the foam samples did not fracture under the first impact, they were subjected to subsequent impact loadings until they fractured or until testing was discontinued. No 40 pcf foam samples survived the second impact loading. The 30 pcf foam samples were all fractured after the fourth impact loading; however, the samples remained as a single material unit. After seven impacts, no fractures were visible in the Sunshine foam samples. Results from the repeated impact tests are presented in Table V.

For all of the foams, the yield stresses and moduli of elasticity decrease with successive impacts whereas the maximum strains increase. The area factors tend to decrease slowly with increasing number of impacts.

Figures 18-21 show Sunshine and 30 pcf foam stress-strain curves for repeated impact tests. Note that for the third impact on Sunshine foam (Fig. 18), strain hardening now occurs (strain softening occurred on first impact). Strain hardening occurs during all subsequent tests on Sunshine foam. Figures 15 and 18-19 clearly show that the stress-strain characteristics of Sunshine foam change considerably when subjected to successive loadings into the inelastic range. Successive tests on 30 pcf foam (Figs. 16 and 20-21) only change the stress-strain curves slightly, the principal differences being the "rounding" effect in the region of the yield stress and the maximum strain. The 40 pcf foam samples displayed fractures after the

first impact. The results of the second impact tests must be highly dependent upon the extent of internal fracturing because these results were erratic and therefore have not been shown.

E. Discussion of Results

The data from drop tests on urethane foams can be described as low-precision data; therefore, to positively establish relationships between variables, some statistical method must be used. Because the number of tests available is small, no statistical analyses of the test results were attempted.

For each urethane foam tested, modulus of elasticity and yield stress versus loading rate are shown in Figs. 22-24. The dashed lines shown in these figures are included to suggest trends only and are not based on any best-fit technique. For all foams, there is a trend toward increasing yield stress and modulus of elasticity as the loading rate increases; however, the percentage increase for each foam is different as illustrated in Table VI. Sunshine foam displays the largest increase in yield stress and modulus of elasticity over the loading rate range from 10 to 324 000 mm/min and 40 pcf foam displays the least increase in these parameters.

Another trend observed from Figs. 22-24, particularly for Sunshine and 40 pcf foams, is the similar pattern between the yield stress and modulus of elasticity data points. This suggests that a relationship between the yield stress and modulus of elasticity exists such that knowing one parameter, the other can be predicted, and the relationship is valid over the entire loading-rate range. More tests would be required to establish this relationship.

The yield stress and modulus of elasticity of the 30 and 40 pcf foams appear to increase linearly (on a log-log plot) with loading rate whereas, for Sunshine foam, these parameters increase more rapidly at the higher loading rates (again on a log-log plot).

For applications in which foams are used as a cushioning media to protect components from impact loadings, the foam's most important behavior property depends upon the protected component characteristics. If displacement of the component is critical, then the foam's modulus of elasticity and yield stress (the higher the better) are its most important properties. If the component is sensitive to high accelerations, then the foam's modulus of elasticity, yield stress, and ability to absorb energy are its important properties. It is assumed that if deflections are not critical, inelastic foam action is permissible. The characteristics of the protected component must be known before the protecting material can be selected.

Even when loaded well beyond its yield stress, Sunshine foam exhibits little permanent deformation; however, both 30 and 40 pcf foams permanently deform upon loading beyond their yield stresses. The permanent deformations of these foams could be used to estimate impact loadings experienced by a prototype component during a test if the input energy versus permanent deformation relationship were known and the foam was loaded beyond its yield stress. The 30 pcf foam would be superior to the 40 pcf foam for this application because of its lower modulus of elasticity and yield stress and because it does not shatter under impact loads.

TABLE V

RESULTS OF REPEATED IMPACT TESTS
Impact Energy - 3.15 MJ/m³

Impact No.	Initial Strain Rate (1/s)	Area Factor	Maximum Strain (mm/mm)	Yield Stress (MPa)	Modulus of Elasticity (MPa)	Test Date
<u>Sunshine Foam</u>						
2	213	0.701	0.178	17.1	371	02-25-85
2	213	0.665	0.200	14.3	393	02-28-85
2	166	0.722	0.209	14.4	340	03-18-85
2	120	0.686	0.196	15.9	381	04-03-85
3	213	0.623	0.216	12.9	347	02-25-85
3	213	0.698	0.187	14.4	527	02-28-85
3	166	0.683	0.246	10.6	338	03-08-85
3	166	0.671	0.235	11.2	222	03-18-85
3	120	0.613	0.251	10.4	247	04-02-85
4	213	0.582	0.233	10.2	292	02-28-85
4	166	0.617	0.265	9.8	179	03-18-85
5	166	0.589	0.288	8.2	148	03-18-85
7	166	0.507	0.366	5.4	181	03-08-85
<u>30 Pcf Stafoam 760</u>						
2	213	0.538	0.157	22.1	410	02-25-85
2	213	0.588	0.190	16.6	301	02-28-85
2	166	0.601	0.220	15.1	274	03-18-85
2	120	0.612	0.178	19.6	376	04-02-85
2	120	0.609	0.205	15.8	302	04-03-85
3	213	0.503	0.178	19.4	383	02-25-85
3	213	0.560	0.216	14.7	196	02-28-85
3	166	0.565	0.226	14.8	196	03-08-85
3	120	0.608	0.192	17.8	293	04-02-85
4	213	0.545	0.223	13.7	160	02-28-85
4	166	0.564	0.230	14.4	184	03-08-85
<u>40 Pcf Stafoam 760</u>						
2	166	0.697	0.172	23.6	408	03-08-85
2	120	0.537	0.114	36.6	741	04-03-85

TABLE VI

NOMINAL LOAD-RATE RESULTS

<u>Loading Rate (mm/min)</u>	<u>Yield Stress (MPa)</u>	<u>Modulus of Elasticity (MPa)</u>
<u>Sunshine Foam</u>		
10	7.5	113
324,000	30.0	500
<u>30 Pcf Stafoam 760</u>		
10	12.0	280
324,000	20.5	480
<u>40 Pcf Stafoam 760</u>		
10	27.0	580
324,000	35.0	640

V. SUMMARY

Quasistatic and drop tests were used to evaluate Sunshine, 30 pcf, and 40 pcf foams when subjected to different loading rates. Quasistatic tests were performed at loading rates from 10 to 9000 mm/min (0.0066 to 5.91 1/s) and drop tests were conducted at loading rates from 182 500 to 324 300 mm/min (120 to 213 1/s).

From the tests and test data, the following observations were made:

1. All three foams displayed increasing yield stresses and moduli of elasticity with increasing loading rates. Sunshine foam displayed the greatest loading rate effect and 40 pcf foam displayed the smallest loading rate effect.
2. All of the foams showed a large energy absorption capacity when loaded beyond their yield stresses.
3. The stress-strain curves for Sunshine foam changed greatly when subjected to repeated impacts with sufficient energy to produce inelastic action.
4. Sunshine foam did not display visible fracture lines in any test, even up to strains exceeding 50%.
5. The 30 pcf foam showed fracture lines after several successive impacts delivering about 3.15 MJ/m³ per impact; however, the samples remained as a single unit. In the quasistatic tests, no fracture lines were visible in samples tested to a strain of 50% and at loading rates up to 500 mm/min; however, fractures were visible when tested to a strain of 59% at a loading rate of 9000 mm/min.

6. The 40 pcf foam showed fracture lines after one impact delivering about 3.15 MJ/m³. In several tests, fragments separated from the sample.

Because of many uncontrollable variables, quasistatic and drop tests on urethane foams yield low-precision data. Testing under strictly controlled conditions may increase the precision of the data, but it cannot result in high-precision data. Because of the scatter in the data, many tests are needed to completely define the mechanical behavior of urethane foams subjected to different load rates. The data now available are sufficient to establish behavior trends that can serve as a guide for planning additional tests.

ACKNOWLEDGMENTS

Appreciation is extended to Cynthia Sandoval, who provided the foam system descriptions and formulations; to Richard Harlow, who conducted most of the quasistatic tests; and to Richard Browning, who provided technical assistance and helped conduct a series of quasistatic tests.

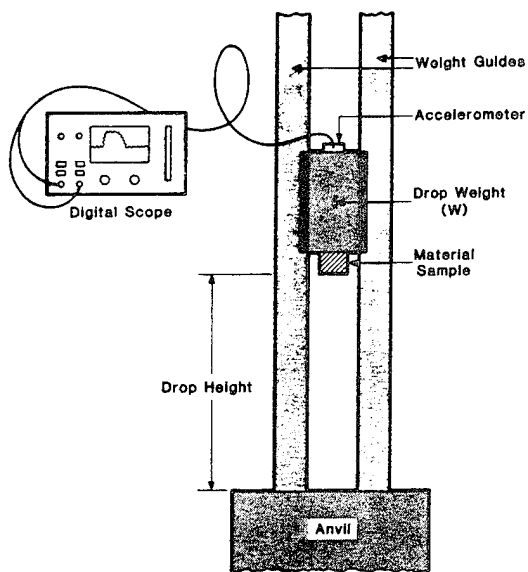


Fig. 1. Drop test set-up.

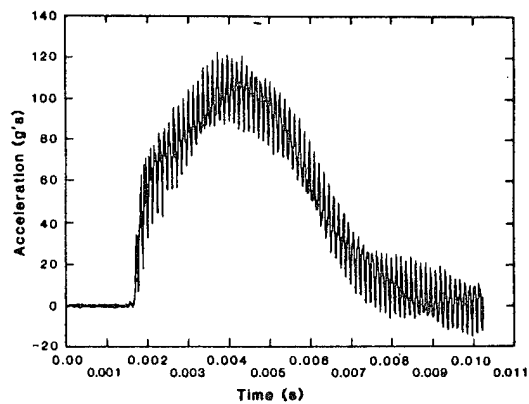


Fig. 3. A measured accelerogram.

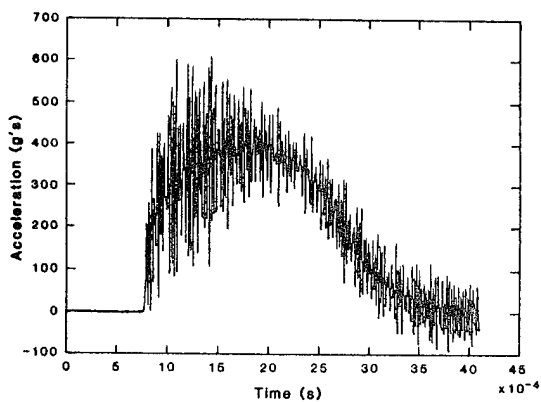


Fig. 2. Acceleration pulse with ringing.

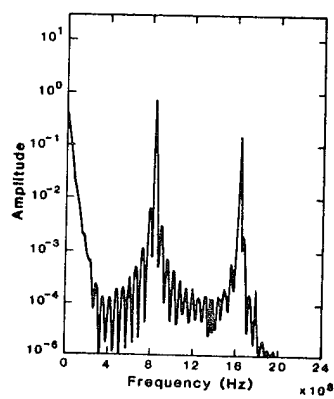


Fig. 4. PSD of measured accelerogram.

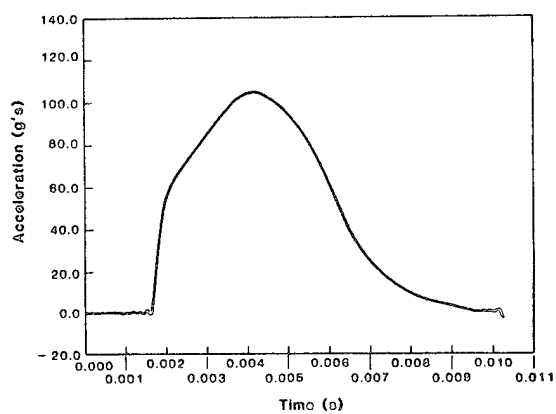


Fig. 5. Filtered accelerogram.

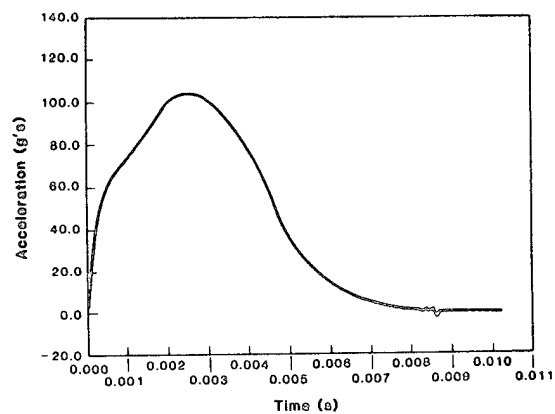


Fig. 7. Time base corrected accelerogram.

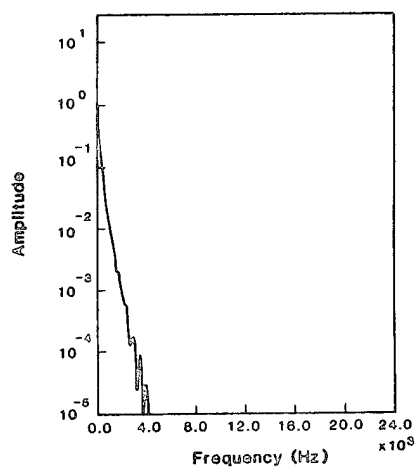


Fig. 6. PSD of filtered accelerogram.

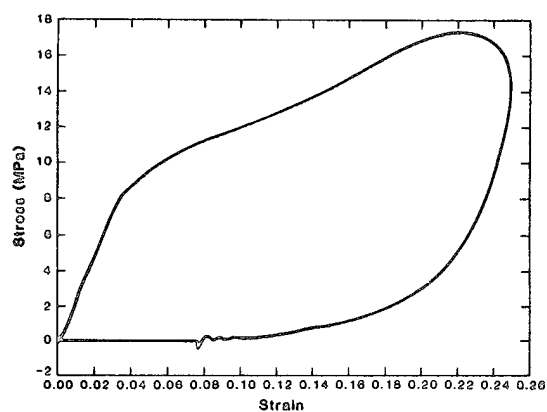


Fig. 8. Stress-strain relationship.

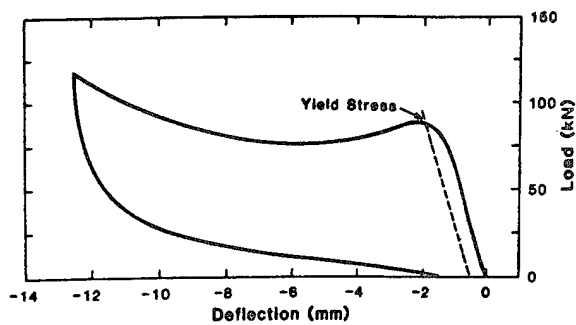


Fig. 9. Load-deflection relationship for Sunshine foam.

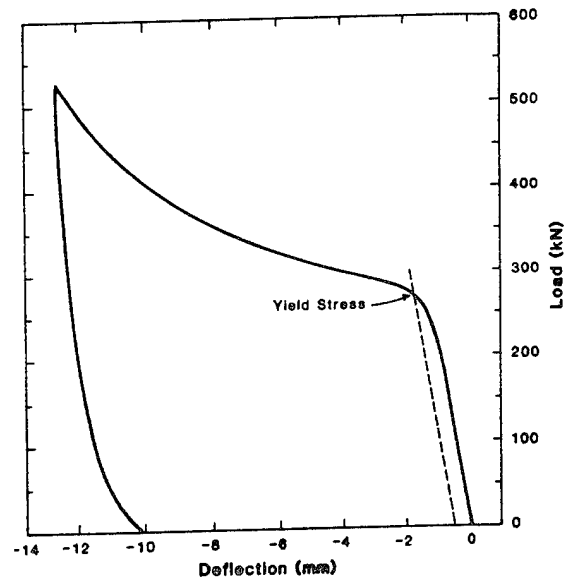


Fig. 11. Load-deflection relationship for 40 pcf foam

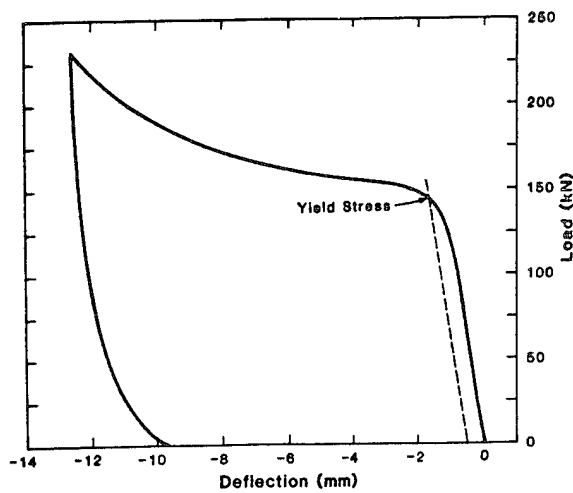


Fig. 10. Load-deflection relationship for 30 pcf foam.

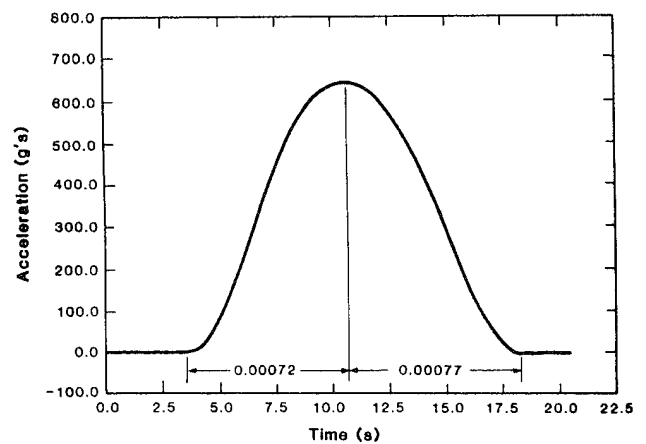


Fig. 12. Test 1 accelerogram - mostly elastic action.

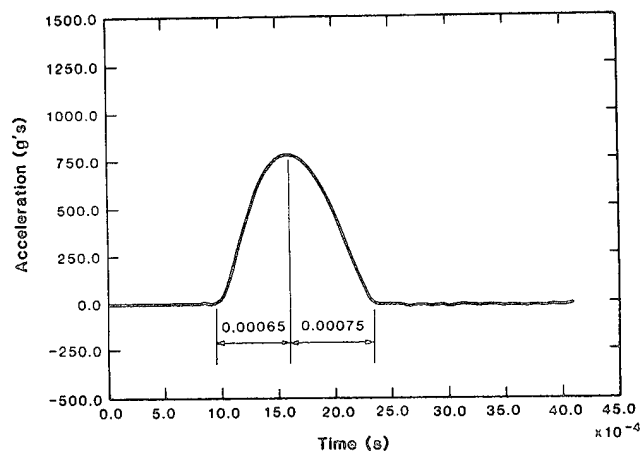


Fig. 13. Test 4 accelerogram - some inelastic action.

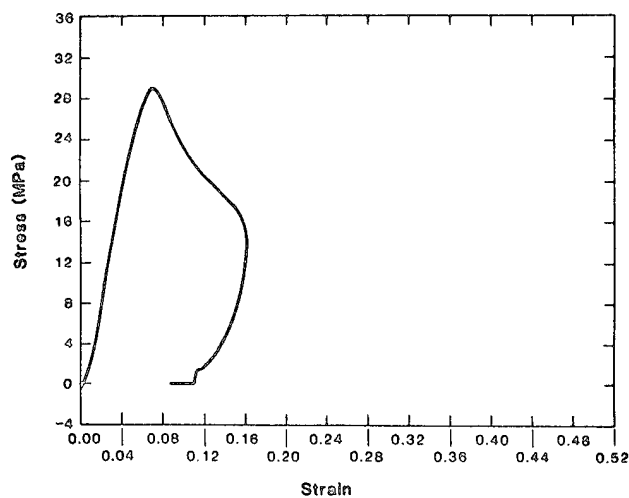


Fig. 15. Sunshine foam stress - strain relationship (Test 1).

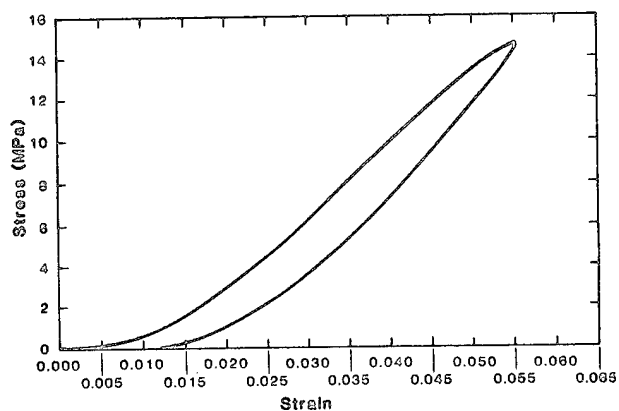


Fig. 14. Stress-strain relationship (Test 1).

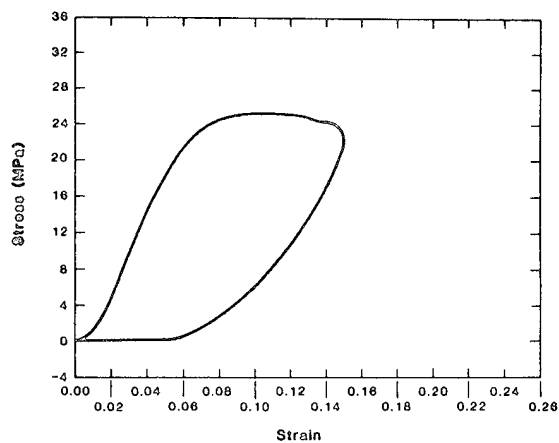


Fig. 16. 30 pcf foam stress-strain relationship (Test 1).

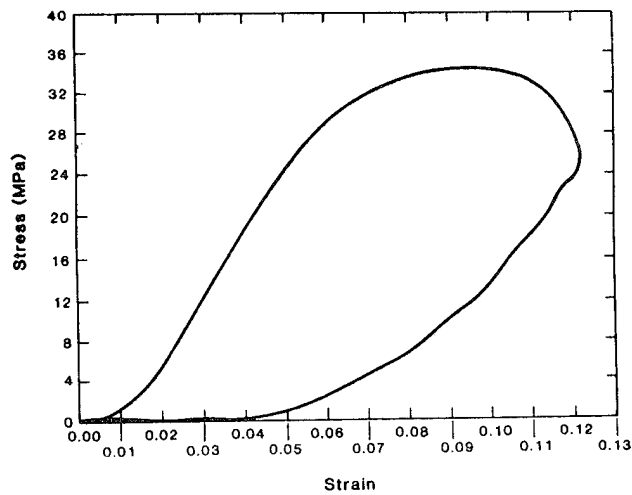


Fig. 17. 40 pcf foam stress-strain relationship.

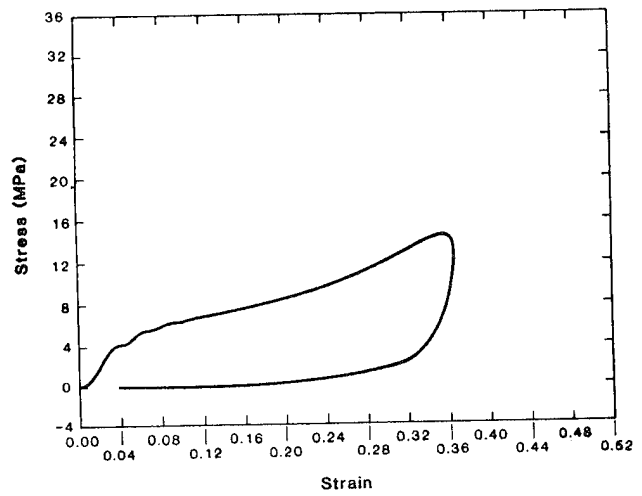


Fig. 19. Sunshine foam stress-strain relationship (Test 7).

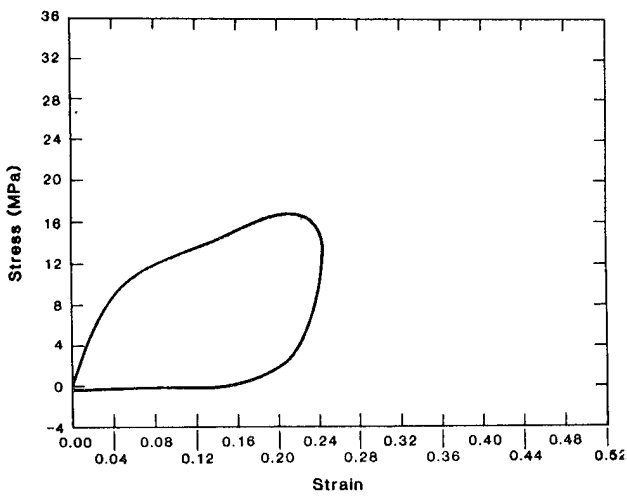


Fig. 18. Sunshine foam stress-strain relationship (Test 3).

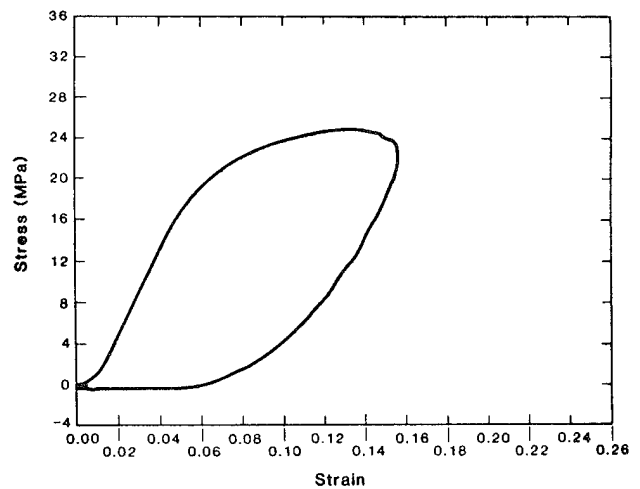


Fig. 20. 30 pcf foam stress-strain relationship (Test 2).

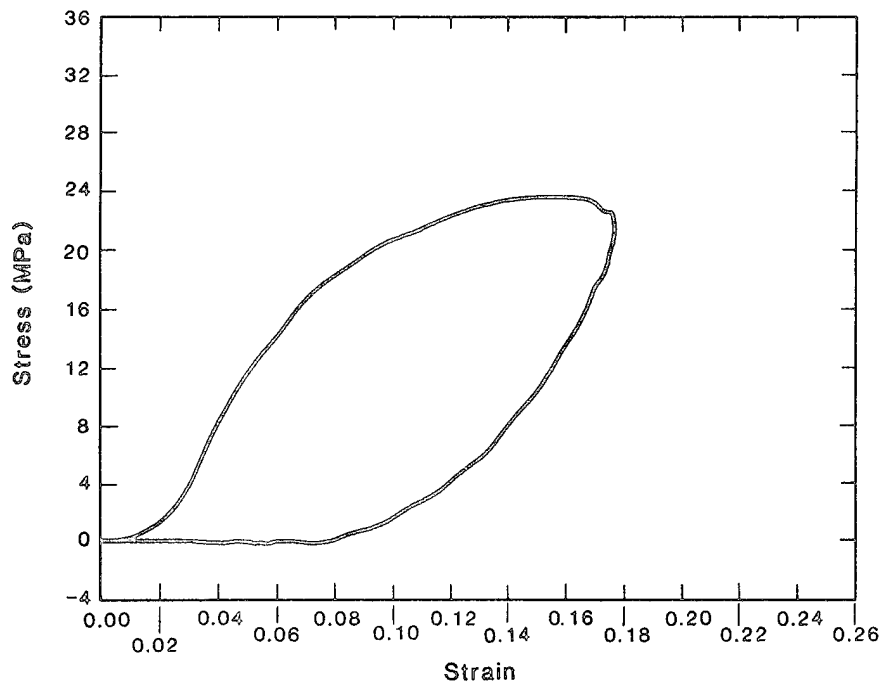


Fig. 21. 30 pcf foam stress-strain relationship (Test 3).

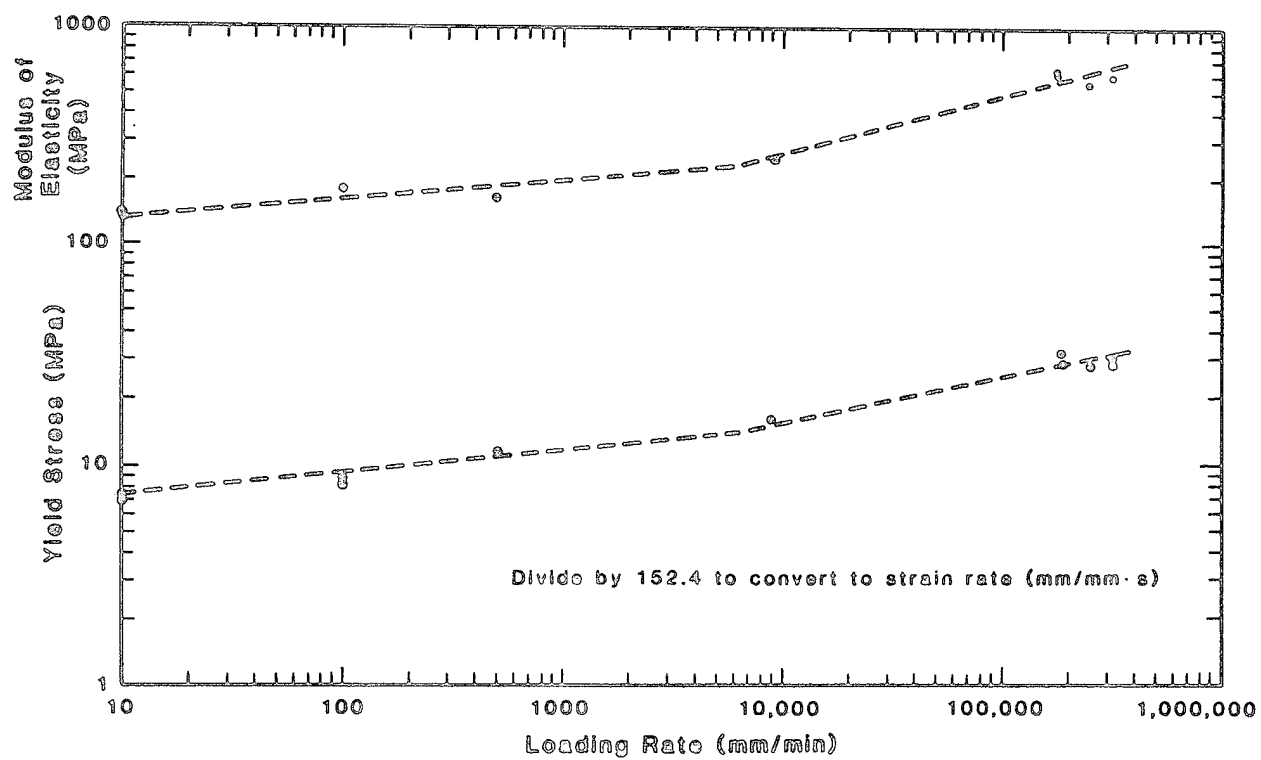


Fig. 22. Sunshine foam load-rate relationships.

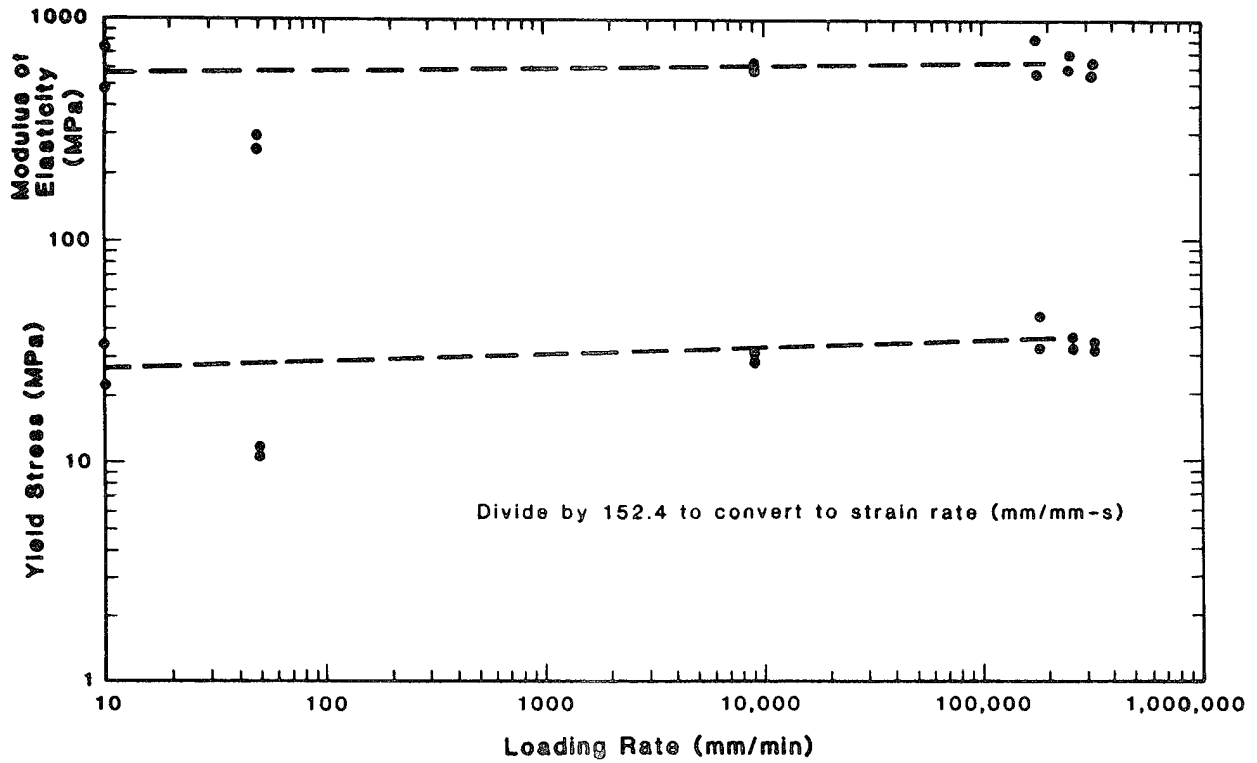


Fig. 23. 30 pcf foam load-rate relationships.

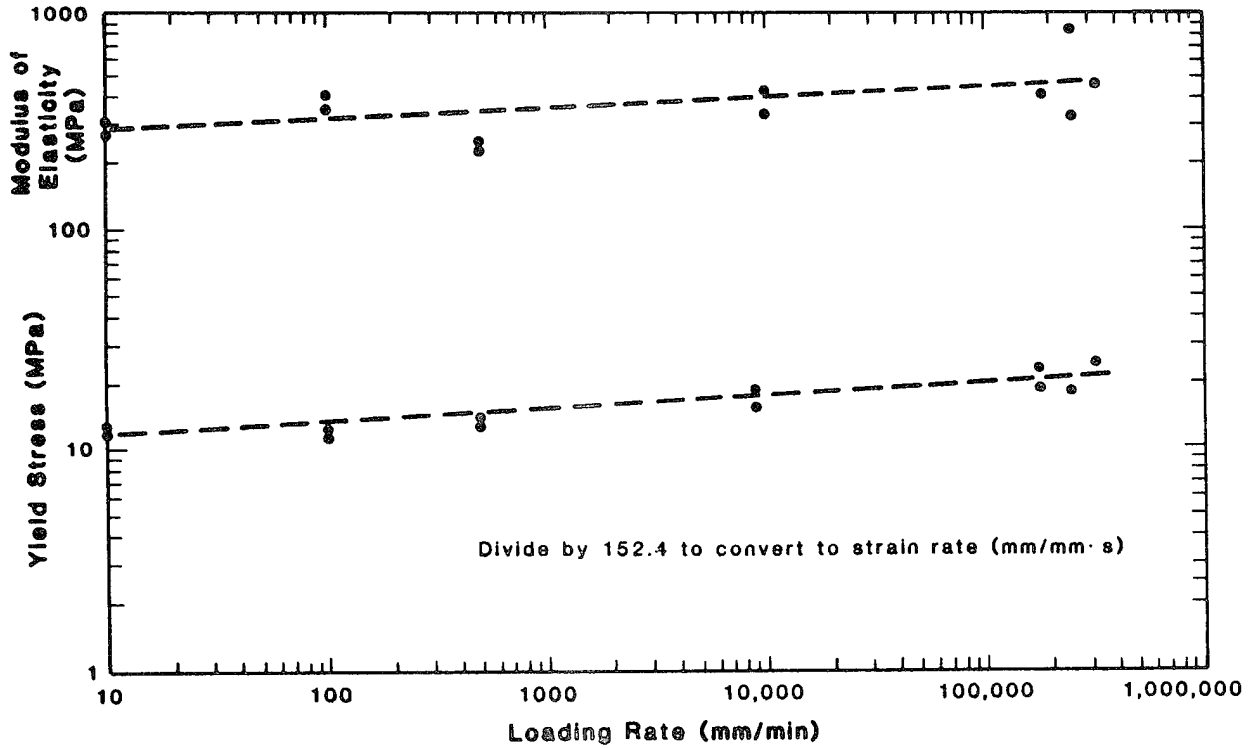


Fig. 24. 40 pcf foam load-rate relationships.

Printed in the United States of America
 Available from
 National Technical Information Service
 US Department of Commerce
 5285 Port Royal Road
 Springfield, VA 22161

Microfiche (A01)

NTIS		NTIS		NTIS		NTIS	
Page Range	Price Code	Page Range	Price Code	Page Range	Price Code	Page Range	Price Code
001-025	A02	151-175	A08	301-325	A14	451-475	A20
026-050	A03	176-200	A09	326-350	A15	476-500	A21
051-075	A04	201-225	A10	351-375	A16	501-525	A22
076-100	A05	226-250	A11	376-400	A17	526-550	A23
101-125	A06	251-275	A12	401-425	A18	551-575	A24
126-150	A07	276-300	A13	426-450	A19	576-600	A25
						601-up*	A99

*Contact NTIS for a price quote.